

- (75) For discussions see (a) R. D. Mattuck, "A Guide to Feynman Diagrams in the Many-Body Problem", McGraw-Hill, New York, 1967, Chapter 15; (b) C. Kittel, "Introduction to Solid State Physics", 4th ed., Wiley, New York, 1971, Appendix L.
- (76) See ref 60, Chapter E.
- (77) For a discussion of the relationship between lattice instability and superconductivity see T. Riste, Ed., "Electron-Phonon Interactions and Phase Transitions", Plenum Press, New York, 1977.
- (78) C. K. Chiang, Y. W. Park, A. J. Heeger, H. Shirakawa, E. J. Louis, and A. G. MacDiarmid, *Phys. Rev. Lett.*, **39**, 1098 (1977); C. K. Chiang, M. A. Dray, S. C. Gau, A. J. Heeger, E. J. Louis, A. G. MacDiarmid, Y. W. Park, and H. Shirakawa, *J. Am. Chem. Soc.*, **100**, 1013 (1978).
- (79) R. L. Greene, G. B. Street, and L. J. Suter, *Phys. Rev. Lett.*, **34**, 577 (1975).
- (80) For a review see H.-P. Geserich and L. Pintschovius, *Adv. Solid State Phys.*, **16**, 65 (1976).

Spin-Orbit Coupling in Metal-Anion Systems. The Colors of Post-Transition Metal Salts

T. P. Carsey[†] and S. P. McGlynn*

Contribution from the Coates Chemical Laboratories, The Louisiana State University, Baton Rouge, Louisiana 70803. Received July 28, 1978

Abstract: A configuration-mixing model is developed for spin-orbit coupling in metal salts. The component excited configurations are of locally excited (LE) or charge transfer (CT) varieties. It is shown that the triplet \leftarrow singlet ($T_1 \leftarrow S_0$) transition of the nominal anion steals its intensity from local excitations in the case of light nontransition metal salts (e.g., NaNO_2) and from charge-transfer excitations in the case of heavy post-transition metal salts (e.g., AgNO_2). The model provides a simple rationalization of the colors and luminescences of post-transition metals in which neither the anion nor cation is separately chromophoric.

Introduction

The external heavy-atom effect is a valuable technique in the study of multiplicity-forbidden electronic transitions.¹ In particular, it has been used to interpret² the colors of post-transition metal salts in which neither the anion nor cation is separately colored. This interpretation, which constitutes a theory of color and luminescence for post-transition metal salts, suffered some defects.

(1) The data were qualitative. In the meantime, a considerable body of information on polarizations and oscillator strengths has been provided by Reznick et al.³⁻⁵

(2) The previous spin-orbital discussions⁶ were "whole-molecule" in nature. The anion and cation systems were treated as a single unit. The resulting MO considerations, while substantiative of theory, were difficult to analyze for physical content.

(3) Too great a reliance was placed on computed quantities. Few experimental checks were available, and the computational results were indiscriminately used in spin-orbit considerations. The danger inherent in such an approach is demonstrated in Figure 1. The various data sets of Figure 1, when used in a perturbation-theory processing of spin-orbit coupling, yield quite different results, which is obviously unsatisfactory.

The present work proposes a rephrasing of the perturbation approach at the configuration, as opposed to the orbital, stage. Recent discussions of such an approach are available.^{1,7,8} There is no doubt, in the present instance anyway, that the configuration mixing model is less satisfactory in a theoretical sense. It simply introduces (or reintroduces) the mixing of cation and anion wave functions at too late a stage and, because of the restricted number of locally excited (LE), charge transfer (CT), and retro-charge-transfer (RCT) configurations which may be considered, the degree of configuration mixing is almost certainly too limited. Nonetheless, the approach has certain advantages. Firstly, it facilitates the use of the empirical data, energies and intensities, which are available for the locally excited states of the anion and cation systems and for the CT

states of the anion/cation system. Secondly, the results are more readily visualized, and may lead to conclusions concerning the origin of singlet-triplet enhancement (i.e., to the relative importance of the external heavy-atom effect in terms of either the spin-orbit coupling which the heavy-atom center mediates or the anion \leftrightarrow cation charge transfer which permits the anion electrons to participate in this coupling). Finally, by virtue of its inclusion of CT configurations at the very outset, it should permit some estimation of the degree, if any, to which anion $T_1 \leftarrow S_0$ transitions steal intensity from charge-transfer transitions.

The Configuration-Interaction (CI) Model

The zero-order wave functions are constructed from four MO functions: the LUMO and HOMO of the metal ion, $\varphi_{m'}$ and $\varphi_{m''}$, respectively, and the LUMO and HOMO of the anion, $\varphi_{a'}$ and $\varphi_{a''}$, respectively. These configurations are diagrammed in Figure 2.

The transition of interest is ${}^3\psi_{\Lambda^*} \leftarrow {}^1\psi_0$. This transition, in zero order, is anion localized and is responsible for the color of post-transition metal salts.² In order for it to acquire transition probability, it must mix, under the influence of spin-orbit coupling engendered at the metal center, with $S_i \leftarrow S_0$ transitions. Consequently, we write the spin-orbit corrected ${}^3\psi_{\Lambda^*}$ function as

$${}^3\Psi_{\Lambda^*} = {}^3\psi_{\Lambda^*} + C_1 {}^1\psi_0 + C_2 {}^1\psi_{\Lambda^*} + C_3 {}^1\psi_{M^*} + C_4 {}^1\psi_{CT} + C_5 {}^1\psi_{RCT} \quad (1)$$

where

$$C_i \ (i = 1, 2, 3, 4, 5) = \langle {}^1\psi_i | \mathcal{H}' | {}^3\psi_{\Lambda^*} \rangle / [E_i^0 - E^0({}^3\Lambda^*)] \quad (2)$$

where \mathcal{H}' is the spin-orbit Hamiltonian and the eigenvalues E_i^0 refer to a nonrelativistic Hamiltonian. The spin-orbit-corrected ground state wave function is

$${}^1\Psi_0 = {}^1\psi_0 + C_6 {}^3\psi_{\Lambda^*} + C_7 {}^3\psi_{M^*} + C_8 {}^3\psi_{CT} + C_9 {}^3\psi_{RCT} \quad (3)$$

The transition moment of interest, ${}^3\Psi_{\Lambda^*} \leftarrow {}^1\Psi_0$, in first order, is

[†] National Institute for Occupational Safety & Health, Robert A. Taft Laboratories, Columbus, Ohio 43226.

Table I. Transition Dipole Moment in MO Format (\mathcal{H}'_z Component Only)

component (cf. eq 4) index i	SOC-corrected wave function	MO expression for \mathbf{M}
1	${}^3\Psi_{A^*} = {}^3\psi_{A^*} + C_1 {}^1\Psi_0$	$-\sqrt{2}\langle a H' a'\rangle[\mu_0 - 2S_{am}\langle a \mathbf{r} m\rangle + \langle m \mathbf{r} a\rangle]/[E^0({}^3A^*) - E_0^0]$
2	${}^3\Psi_{A^*} = {}^3\psi_{A^*} + C_2 {}^1\Psi_{A^*}$	$\sqrt{2}[-\langle a' H' a'\rangle + \langle a H' a\rangle][\langle a \mathbf{r} a'\rangle - S_{a'm}\langle a \mathbf{r} m\rangle - S_{am}\langle m \mathbf{r} a\rangle]/[E^0({}^3A^*) - E^0({}^1A^*)]$
3	${}^3\Psi_{A^*} = {}^3\psi_{A^*} + C_3 {}^1\Psi_{M^*}$	$\sqrt{2}[S_{am}\langle m' H' a\rangle + S_{a'm'}\langle a H' m\rangle][\langle m \mathbf{r} m'\rangle - S_{am'}\langle m \mathbf{r} a\rangle - S_{am}\langle a \mathbf{r} m\rangle]/[E^0({}^3A^*) - E^0({}^1M^*)]$
4	${}^3\Psi_{A^*} = {}^3\psi_{A^*} + C_4 {}^1\Psi_{CT}$	$\sqrt{2}[S_{a'm'}\langle m' H' m\rangle + S_{a'm'}\langle a H' a\rangle - S_{am'}\langle a H' a'\rangle][\langle a \mathbf{r} m'\rangle - S_{am'}\langle m \mathbf{r} m'\rangle + S_{am'}\langle a \mathbf{r} a\rangle + 2S_{am'}\langle m \mathbf{r} m\rangle]/[E^0({}^3A^*) - E^0({}^1CT)]$
5	${}^3\Psi_{A^*} = {}^3\psi_{A^*} + C_5 {}^1\Psi_{RCT}$	$-\sqrt{2}S_{am}[\langle a H' a\rangle + \langle m H' m\rangle - \langle a' H' a'\rangle][\langle m \mathbf{r} a'\rangle - S_{am}\langle a \mathbf{r} a'\rangle + S_{a'm}2\langle a \mathbf{r} a\rangle + \langle m \mathbf{r} m\rangle]/[E^0({}^3A^*) - E^0({}^1RCT)]$
6	${}^1\Psi_0 = {}^1\psi_0 + C_6 {}^3\Psi_{A^*}$	$-\sqrt{2}\langle a' H' a\rangle[\mu_{A^*} - S_{am}\langle a \mathbf{r} m\rangle + \langle m \mathbf{r} a\rangle] - S_{a'm}\langle a' \mathbf{r} m\rangle + \langle m \mathbf{r} a'\rangle]/[E_0^0 - E^0({}^3A^*)]$
7	${}^1\Psi_0 = {}^1\psi_0 + C_7 {}^3\Psi_{M^*}$	$-\sqrt{2}\langle m' H' m\rangle[-S_{am}\langle a' \mathbf{r} m'\rangle - S_{a'm'}\langle m \mathbf{r} a\rangle]/[E_0^0 - E^0({}^3M^*)]$
8	${}^1\Psi_0 = {}^1\psi_0 + C_8 {}^3\Psi_{CT}$	$\sqrt{2}[S_{am'}\langle a H' a\rangle + S_{am'}\langle m' H' a\rangle][\langle m' \mathbf{r} a'\rangle - S_{am'}\langle a \mathbf{r} a'\rangle - 2S_{a'm'}\langle m \mathbf{r} m\rangle + S_{a'm}\langle a \mathbf{r} a\rangle - S_{a'm}\langle m' \mathbf{r} m\rangle]/[E_0^0 - E^0({}^3CT)]$
9	${}^1\Psi_0 = {}^1\psi_0 + C_9 {}^3\Psi_{RCT}$	$\sqrt{2}[S_{a'm}\langle m H' m\rangle + S_{am}\langle a' H' a\rangle][\langle a \mathbf{r} m\rangle + S_{am}\langle a \mathbf{r} a\rangle + \langle a' \mathbf{r} a'\rangle + \langle m \mathbf{r} m\rangle]/[E_0^0 - E^0({}^3RCT)]$

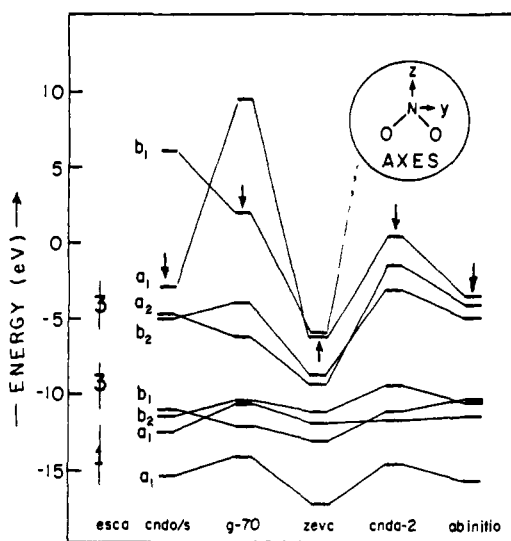


Figure 1. Orbital energies and axes for the nitrite ion. The molecular geometry is taken from crystal-structure data (ref 24). The ab initio results are taken from Wyatt et al.²⁷ The ESCA experimental data refer to LiNO_2 .²⁸ The leftmost vertical lines represent the approximate half-widths of the ESCA bands. The numbers on these lines are the estimated number of molecular orbital excitations in each band. The CNDO/2, CNDO/s, and Gaussian-70 calculations were processed using QCPE Programs 141, 174, and 236, respectively. The ZEV-C65 program is a version of an extended Hückel calculation²⁹ which uses the orbital exponents of Clementi.³⁰ The lowest energy unoccupied MO (i.e., LUMO) of the CNDO/2 calculation was too high in energy (17.29 eV) to be included on the diagram. The highest energy occupied MO (i.e., HOMO) of the ground-state electron configuration is denoted by an arrow. Ab initio SCF calculations are also available in the recent work of Wahl.³¹

$$\mathbf{M} = \sum_{i=1}^5 C_i \left({}^1\psi_i \left| \sum_j \mathbf{e}_j \right| {}^1\psi_0 \right) + \sum_{i=6}^9 C_i \left({}^3\psi_i \left| \sum_j \mathbf{e}_j \right| {}^3\psi_{A^*} \right) \quad (4)$$

where

$$C_i \quad (i = 6, 7, 8, 9) = \langle {}^3\psi_i | \mathcal{H}'_z | {}^1\psi_0 \rangle / (E_i^0 - E_0^0) \quad (5)$$

The first term of eq 4 describes the mixing of singlet states into ${}^3\psi_{A^*}$ while the second describes the mixing of triplets into ${}^1\psi_0$.

The spin-orbit Hamiltonian may be approximated¹ as

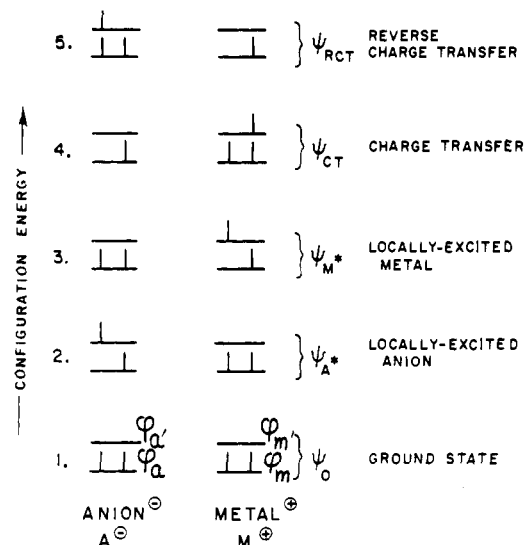


Figure 2. An illustration of the five generic configuration wave functions. The energy scale is suggestive. The salt is designated A^-M^+ for convenience. The upper MO of any pair is the LUMO and the lower is the HOMO.

$$\mathcal{H}' = \sum_{N,j} \xi_N l_j \cdot s_j \quad (6)$$

where the indexes N and j run over atomic centers and electrons, respectively; l and s are orbital and spin angular momentum operators, respectively; and ξ is an empirical spin-orbit coupling constant for which values are available.⁹ The effects of the l and s operators are known.^{1,10} (For example, the l_q ($q = x, y, z$) operators annihilate the s AOs, rotate the p AOs, and have a more complicated effect¹⁰ on the d and f AOs). The configurational expressions for \mathbf{M} may now be reduced¹⁰ to one-electron MO format, the anion-metal overlap being incorporated using Lowdin's method for nonorthogonal basis sets.¹¹ The results for the $M_S = 0$ components of the triplet states are given in Table I. The results for the $M_S = \pm 1$ triplet components are not shown since they differ from those of Table I only by small numerical constants.¹⁰

The symbol S_{am} of Table I refers to a member of the set of overlap integrals $\{\langle a|m\rangle\}$, $S_{a'm'}$ to $\{\langle a|m'\rangle\}$, etc. The inclusion

of these overlaps is forced by the nonorthogonality of the metal orbital set to the anion orbital set. Because of this nonorthogonality, the matrix element of a one-electron operator ρ with respect to two Slater determinants U and V built from such orbitals is¹¹

$$\langle U/\rho/V \rangle = \sum_{k,l} \langle k/\rho/l \rangle D_{UV}(k, l) \quad (7)$$

where k is an orbital element of U , l is an orbital element of V , and $D_{UV}(k, l)$ is the minor of the overlap matrix $\langle U/V \rangle$ obtained by striking out the k th row and l th column.

The simple four-orbital model based on the set $\{\varphi_m, \varphi_{m'}, \varphi_a, \varphi_{a'}\}$ is too restrictive. Hence, in Table I, we extend the meaning of the symbol a so that it represents the set of *all* filled MOs of the ground configuration of A^- , say $\{a_0, a_1, a_2, \dots\}$; similarly, a' now represents the set of *all* unfilled MOs of the ground configuration of A^- , say $\{a'_0, a'_1, a'_2\}$. Similar extensions of the symbols m and m' are also implied (i.e., $m \equiv \{m_0, m_1, m_2, \dots\}$ and $m' \equiv \{m'_0, m'_1, m'_2, \dots\}$). In view of this extension, it is well to emphasize that the ${}^3\psi_{A^*}$ configuration excitation (which, here, is held responsible for the colors of the post-transition metal salts) is always understood to be of configurational type $a_0 \rightarrow a'_0$ in expressions 1–5, whereas in expression 6 it may represent *any* triplet configuration of type $a_i \rightarrow a'_j$. Consequently, each of the expressions 1–9 of Table I actually comprises a set of expressions which may be denoted $\{1\}, \{2\}, \dots, \{9\}$ and which may be referred to as “CT”, “anion localized”, “RCT”, etc.

Results of the Model

If we neglect overlap (i.e., define all $S = 0$), Table I simplifies considerably. Components 3, 4, 5, 7, 8, and 9 go to zero, indicating that the only spin-orbit mixings of significance are those involving pure anion states. Such a model cannot account for the observed effects induced by the metal ion. Hence, a zero-overlap model is inadequate.

The inclusion of overlap, unfortunately, yields a very complex tabulation (cf. Table I). Thus, certain reasonable approximations must be made in order to simplify Table I. These follow.

(1) Second-order terms in S are neglected.

(2) All two center spin-orbit coupling terms (e.g., $\langle a|\mathcal{H}'|m \rangle$) are neglected because of the $1/r^3$ dependence of such matrix elements. In justification of this neglect, we observe that the two-center one-electron terms based on the operator of eq 6 are found to be no larger than $\sim 10\%$ of the one-center one-electron terms for the case of first- and second-row diatomic molecules.¹² In addition, it has been found that the two-center one-electron (from eq 6) and the two-center two-electron contributions (from spin-orbit coupling) tend to cancel.^{12,13} Hence, within the context of the approximations implicit in the configuration-mixing model and those involved in using eq 6, it is justifiable to neglect all two-center terms ($\langle a|\mathcal{H}'|m \rangle$, $\langle a'|\mathcal{H}'|m \rangle$, etc.).

(3) Since \mathcal{H}' may not mix functions with different angular momentum quantum numbers, we may neglect all matrix elements $\langle m|\mathcal{H}'|m' \rangle$ because we have, for energetic reasons, confined the set $\{m\}$ to the metal nd orbitals and the set $\{m'\}$ to the metal $(n+1)s$ and $(n+1)p$ orbitals. In the case of sodium, $\{m\}$ corresponds to the metal $2p$ orbitals and $\{m'\}$ to metal $3s$ and $3p$ orbitals. The corresponding integrals $\langle m|\mathcal{H}'|m' \rangle$ are zero because of principal quantum number orthogonality.

(4) Since \mathcal{H}' does not usually transform as the totally symmetric representation (in particular, it does not do so in C_{2v}), any integral of the form $\langle k|\mathcal{H}'|l \rangle$, where $k = l$, is zero.

With these identities and assertions, we may deduce some qualitative conclusions from Table I.

(a) Expressions 3 and 7 go to zero. Consequently, we expect that intensity stealing from local metal excitations, such as $nd \rightarrow (n+1)s$ and $nd \rightarrow (n+1)p$, or $np \rightarrow (n+1)s$ and $(n+1)p$, will be small. In view of the second-order nature of these terms, we neglect them outright.

(b) Expressions 2 contain no spin-orbit coupling on the metal center. Consequently, their values are expected to be small. This indeed is found to be the case for all MO basis sets of Figure 1. However, while these contributions may usually be neglected in the case of heavy-metal salts, they assume dominant importance in the *isolated* anion and in its *light*-metal salts. Furthermore, since the expressions 2 do not permit exposure of the large spin-orbit coupling available on the metal site, we can expect that they will be unable to account for the increase of this coupling which ostensibly occurs in a heavy-metal salt such as $\text{Pb}(\text{NO}_2)_2$. In sum, while these terms are usually small, they may not be neglected prior to evaluation and inspection, since situations can occur (i.e., the existence of near degeneracies and their association with transitions of large oscillator strengths) which can render their contributions unexpectedly large.¹⁴

(c) The sum of expressions 1 and 6 is

$$\mathbf{M} = \sqrt{2} \langle \varphi_{a'} | \mathcal{H}'_z | \varphi_a \rangle (\mu({}^3A^*) - \mu_0) / \times [E_0^0 - E^0({}^3A^*)] \quad (8)$$

which describes an intensity conferral by the change of static dipole moment between the ${}^3\Psi_{A^*}$ and ${}^1\Psi_0$ states. Such a mechanism for the enhancement of the $T_1 \leftarrow S_0$ transition intensities of organic nonionic materials has been discussed previously.^{1,15} We consider this contribution to be important only when the $T_1 \leftarrow S_0$ transition is of dominant charge-transfer character. In sum, (1), the integral $\langle \varphi_{a'} | \mathcal{H}'_z | \varphi_a \rangle$ contains no spin-orbit coupling terms from the metal center; (2) the difference $\mu({}^3A^*) - \mu_0$ may well be small even though the individual μ_i are large; and (3) numerical evaluation for AgNO_2 produces values that are too small relative to experiment.

In an effort to provide some “feel” for the magnitude of these contributions, we now indulge some qualitative considerations. Suppose that the ${}^3\psi_{A^*} \leftarrow {}^1\psi_0$ transition is of 50% CT character. In other words, suppose that this transition is accompanied by the displacement of one-half an electron from the anion to the cation. The resulting change in dipole moment, given structure 1 of Figure 3, is $\mu({}^3A^*) - \mu_0 \simeq k2.8 \text{ D}$. For the nitrite system, this produces a transition moment $M_z = 3.432 \times 10^{-3} \text{ D}$. Thus, the transition is predicted to be solely z polarized, which it is not. Furthermore, the ${}^3\psi_{A^*} \leftarrow {}^1\psi_0$ transition must now be viewed as heavily CT and, consequently, the energy of this transition, in order to account for variations of the oscillator strength with cation, must vary as the electron affinity of the cation—which, again, it does not. Finally, while the quoted value of M_z is not small, it is no larger than the general run of the other terms arising from expressions 4, 5, 8, and 9 (vide infra).

The extent of CT could, of course, be larger than 50%. But the required variation of % CT needed to account for the observed variations of oscillator strength is inconsistent with the energy invariance of the transition in question. Consequently, while expressions 1 and 6 may not be blithely neglected, there is reason to suppose that they are not the dominating spin-orbital contributions.

(d) Expressions 5 and 9, via the term $\langle \{m\} | \mathcal{H}' | \{m\} \rangle$, contain spin-orbit coupling on the metal center and they steal intensity from the RCT transition. These terms, consequently, will be large. However, in view of the large energies which one might expect for the RCT energy, denominator considerations will reduce their magnitude considerably. Indeed, if it were not for denominator magnitudes, these terms would dominate Table I for the case of heavy-metal salts.

Table II. Components of 3B_1 (and 3A_2) in C_{2v}

spin part	space part	space + spin part	transition moment polarization
T_x, B_2	$B_1(A_2)$	$A_2(B_1)$	forbidden (x)
T_y, B_1	$B_1(A_2)$	$A_1(B_2)$	z (y)
T_z, A_2	$B_1(A_2)$	$B_2(A_1)$	y (z)

Expressions 4 and 8 do not contain spin-orbit coupling on the metal center. However, they steal intensity from the CT transition which, like the RCT transition, will be of high oscillator strength but which, unlike the RCT transition, will be of low energy. Indeed, in the case of heavy metal salts, the energy denominator $E({}^3\psi_a) - E({}^1CT)$ can approach zero, in which case these terms can become very large indeed.

The qualitative conclusions of the previous points (a), (b), (c), and (d) can be synopsized as follows.

Expressions 3 and 7 are zero; expressions 1, 2, and 6 will dominate in the light-metal salts, although, in this instance, 4 and 8 may not be disregarded; expressions 4, 5, 8, and 9 will dominate in the heavy-metal salts, (4) and (8) being important only when there exist low-energy CT states which lie in the vicinity of the T_1 anionic state.

A Synopsis of Experiment

We restrict ourselves to nitrite salts because the data base is both precise and elaborate. (The general run of post-transition metal salts will be surveyed elsewhere.)¹⁶ The group-theoretic expectations for two possible assignments of the emissive triplet state are summarized in Table II.

Aqueous solutions of nitrite salts exhibit four transitions¹⁷ at energies less than $50 \times 10^3 \text{ cm}^{-1}$: an intense ${}^1\Gamma_{\pi\pi^*} \leftarrow {}^1\Gamma_1$ transition at 210 nm (${}^1B_2 \leftarrow {}^1A_1$), two ${}^1\Gamma_{\pi\pi^*} \leftarrow {}^1\Gamma_1$ transitions at 350 (${}^1B_1 \leftarrow {}^1A_1$) and 290 nm (${}^1A_2 \leftarrow {}^1A_1$), and a ${}^3\Gamma_{\pi\pi^*} \leftarrow {}^1\Gamma_1$ transition at 450 nm (${}^3B_1 \leftarrow {}^1A_1$). In the NaNO_2 crystal, the ${}^3B_1 \leftarrow {}^1A_1$ transition is largely y polarized and, consequently, the zero-field emissive spin state is largely the T_z, A_2 component.^{8,9} The absence of non-totally-symmetric vibrations in the $T_1 \leftarrow S_0$ spectrum^{18,19,20} suggests that a first-order spin-orbit mechanism—and not a second order vibronic-spin-orbit mechanism²¹—is operative.

Considerable changes occur in the heavy-metal salts.

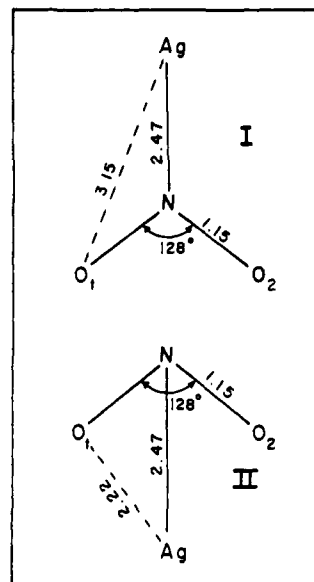
(1) The $T_1 \leftrightarrow S_0$ transition probability increases considerably.² Compared with NaNO_2 , the probability increases²⁻⁵ by three orders of magnitude in $\text{NaAg}(\text{NO}_2)$ and four orders of magnitude in $\text{NaTl}(\text{NO}_2)_2$.

(2) Low-energy charge transfer transitions occur.⁶ An intense z -polarized transition is observed³⁻⁵ at 400 nm in $\text{AgNa}(\text{NO}_2)_2$ and a (y, z) -polarized transition is observed³⁻⁵ at 390 nm in AgNO_2 . An additional z -polarized CT transition is observed^{3,4,5} at 310 nm in AgNO_2 .

Table III. Calculated Transition Probabilities^{a,b}

expression (Table I)	$\text{NaNO}_2, {}^3B_1 \leftrightarrow {}^1A_1$		$\text{AgNa}(\text{NO}_2)_2, {}^3B_1 \leftrightarrow {}^1A_1$		$\text{AgNO}_2, {}^3A_2 \leftrightarrow {}^1A_1$		
	M_y	M_z	$M_z(\text{I})$	$M_z(\text{II})$	$M_x(\text{II})$	$M_y(\text{II})$	$M_z(\text{II})$
1		-6.139×10^{-4}					
2	1.259×10^{-4}	4.461×10^{-4}					
3							
4	4.012×10^{-4}	4.228×10^{-4}	9.217×10^{-3}	2.549×10^{-2}		-1.597×10^{-3}	2.052×10^{-2}
5			-1.662×10^{-3}	-3.178×10^{-3}	-1.093×10^{-3}	-2.076×10^{-2}	1.411×10^{-2}
6	5.100×10^{-4}	5.484×10^{-4}					
7							
8		1.23×10^{-4}	1.784×10^{-3}	-1.833×10^{-3}	8.589×10^{-4}		3.873×10^{-3}
9			7.204×10^{-4}	1.740×10^{-3}	5.199×10^{-5}	-1.848×10^{-4}	-3.073×10^{-3}
$ M_q, \text{total} $	1.37×10^{-3}	9.325×10^{-4}	1.01×10^{-2}	2.22×10^{-2}	1.82×10^{-4}	2.25×10^{-2}	2.77×10^{-2}
$f(\text{calcd})$	2.59×10^{-7}	2.10×10^{-7}	2.44×10^{-5}	1.19×10^{-4}	8.18×10^{-9}	1.25×10^{-4}	1.89×10^{-4}
$f(\text{obsd})$	$\sim 1.0 \times 10^{-7}$	$(10^{-7}), 10^{-8}$	1.1×10^{-4}	1.1×10^{-4}	7×10^{-4}	3×10^{-4}	0.7×10^{-4}

^a The structure, I or II of Figure 3, is shown in parentheses. ^b All values of M not shown are either zero or too small to be significant.

**Figure 3.** The two closest Ag-nitrite orientations in AgNO_2 . The silver lies, in both instances, on the C_2 axis.

(3) The $T_1 \leftarrow S_0$ absorption band of NaNO_2 is polarized^{18,19} along y . In $\text{TlNa}(\text{NO}_2)_2$ the extinction coefficient distribution⁴ is $\epsilon_y > \epsilon_z$, and in $\text{AgNa}(\text{NO}_2)_2$ the polarization⁵ is totally along z . These three sets of data agree with a 3B_1 assignment for T_1 . In AgNO_2 , however, the absorption³ and emission²² contain all three polarizations, the absorption distribution being $\epsilon_x > \epsilon_y > \epsilon_z$. Thus, in the AgNO_2 crystal, at least four possibilities occur: the T_1 state is 3A_2 (see Table II); or the site geometry is not C_{2v} ; or vibronic coupling is manifestly strong; or the x intensity is wrongly attributable to the $T_1 \leftarrow S_0$ transition. In the case of correctness of any of the latter three assertions, the proper assignment for the $T_1 \leftarrow S_0$ transition could also be 3B_1 (or its counterpart in some lower symmetry point group).

Results of Calculations

Sodium Nitrite (NaNO_2). The site symmetry²³ of NaNO_2 is C_{2v} . The $T_1 \leftarrow S_0$ transition is ${}^3B_1 \leftarrow {}^1A_1$. The results of transition probability calculations are given in Table III. The calculated and observed oscillator strengths are in reasonable agreement. As expected, the transition probability is largely uninfluenced by the metal. Indeed, the calculated NaNO_2 values are almost identical with those for the isolated nitrite ion. The same conclusion follows from "supermolecule" MO considerations.⁶

A z -polarized intensity is also predicted. This predicted intensity originates from orbitals dominated by sodium AOs (i.e., the a_1 MOs). Computations suggest that these orbitals are of low energy, whereas experiment indicates otherwise. Consequently, we infer that the computed z moment is an artifact of the computation (i.e., a poor rendition of MO energies). In any event, the z intensity of the observed transition is at least five times lower than that predicted.

AgNa(NO₂)₂. The AgNa(NO₂)₂ crystal exhibits a first-order spin-orbit enhancement of the ${}^3B_1 \leftarrow {}^1A_1$ transition of the nitrite ions. We suppose that this enhancement is "stolen" from a ${}^1A_1 \leftarrow {}^1A_1$ charge transfer band which is not observed in NaNO₂. We now subject these calculations to numerical test.

The crystal structure²⁴ of AgNO₂ suggests two closest Ag-nitrite orientations. These are shown in Figure 3. The integrals of expressions 4, 5, 8, and 9 were evaluated using supermolecule extended Hückel calculations²⁵ for structures I and II. Considerable metal-anion mixing exists in AgNO₂, particularly in structure II—a fact attributed to the smaller Ag-O distance found in II.

Since the active spin component of AgNa(NO₂)₂ is $T_1(B_1)$, we investigate the \mathcal{H}'_x form of (4), (5), (8), and (9) with emphasis on the "stealing" of z -polarized intensity. The results are given in Table III. The energy denominators are experimental and are ${}^3\Psi_{A_1} \leftarrow {}^1\Psi_0$, 2.76 eV, z polarized; ${}^1,{}^3\Psi_{CT} \leftarrow {}^1\Psi_0$, 3.1 eV, z polarized; and ${}^1,{}^3\Psi_{RCT} \leftarrow {}^1\Psi_0$, 4.0 eV, z polarized. Since the singlet-triplet intervals for the charge-transfer transitions (${}^1CT/{}^3CT$) are expected to be small,⁷ we take them to be zero.

The calculated and experimental oscillator strengths of Table III are in good agreement, particularly for structure II. It is clear that the model can account for the preeminent experimental fact of \sim three orders of magnitude increase in the $T_1 \leftarrow S_0$ oscillator strength of AgNa(NO₂)₂ relative to NaNO₂.

AgNO₂. Experimental evidence for a 3A_2 assignment of the T_1 state of AgNO₂ exists. We now apply the spin-orbit coupled configuration model to a 3A_2 state of AgNO₂. We question whether a 3A_2 assignment rationalizes the polarization behavior of AgNO₂ (see Table II).

A ${}^3A_2 \leftarrow {}^1A_1$ transition should exhibit all three polarizations. Therefore, we calculated all spin-orbit coupling and transition moment integrals implicit in expressions 4, 5, 8, and 9. These results are given in Table III for structure II.

The calculated transition moments, while excellent for y and z polarization, yield an x intensity which is much too small. Inclusion of the other expressions 1, 2, and 6 does not alter the values of f_z (calcd) and f_y (calcd) in any significant way, while changing f_x (calcd) to 4.5×10^{-6} , which is still three orders of magnitude too low. The difficulty is not that spin-orbit coupling is small; in fact, the x intensity of a ${}^3A_2 \leftarrow {}^1A_1$ transition derives from very large spin-orbit coupling via \mathcal{H}'_x [e.g., $\langle 2b_2 | \mathcal{H}'_x | 2a_1 \rangle = 826 \text{ cm}^{-1}$, reflective of a large silver d_{yz} -amplitude in the nitrite $2b_2$ MO]. The difficulty is that all out of plane intensities which, under the influence of \mathcal{H}'_x , mix into the ${}^3A_2 \leftarrow {}^1A_1$ transition are all quite small. Thus, while the computations suggest a way out of this difficulty (i.e., augment the intensity of the out of plane transitions from which intensity is stolen), we can find no justification for so doing.

One may conclude that the 3A_2 assignment is wrong; however, the only other reasonable alternative, namely, 3B_1 , is even worse since it requires f_z (calcd) = 0. Consequently, we are led to one of four conclusions: (1) Vibronic considerations based on out of plane vibrational perturbations are important.²⁶ (2) The site symmetry is less than C_{2v} (i.e., the AgNO₂ "molecule" is bent).²⁶ (3) The data/and or assignments are in error. (4) Our calculations underestimate the extent of d -orbital involvement in the ground-state MOs of AgNO₂.

The intensification of the $T_1 \leftarrow S_0$ transition in AgNO₂ (relative to NaNO₂ or NO₂⁻) is reproduced computationally. Unfortunately, the origin of the x -polarized intensity of the $T_1 \leftarrow S_0$ transition is not resolved. Indeed, given the assigned absence of $S_1 \leftarrow S_0$ x -polarized intensity in the crystal spectrum, it seems better to assert that the assigned x -polarized $T_1 \leftarrow S_0$ transition component is more properly identified as an $S_1 \leftarrow S_0$ transition.

Conclusions

Despite the single discrepancy (i.e., x intensity in AgNO₂) we can conclude that the configuration model has considerable validity. As such, we can use it to obtain insight into the sources of triplet intensity and the origins of its enhancement in the heavy-metal salts. These insights follow.

(1) The source of triplet intensity in the light metal salts is almost entirely attributable to expressions 1, 2, and 6. The introduction of mixing with CT states is not necessary in order to obtain reasonable agreement with experiment.

(2) The source of triplet intensity in the heavy-metal salts is almost entirely attributable to expressions 4, 5, 8, and 9. The intensity stealing is attributable to two dominant factors: spin-orbit mixing on the heavy-metal center and the presence of nearby states, CT and RCT, of high transition probability. Expressions 4 and 8 are highly dependent on the latter characteristic and will become small when T_1 and CT states are energetically disparate. It is for this reason that these terms are small in the light-metal salts. Expressions 5 and 9 steal intensity from RCT states which are of quite high energy in all cases but, despite this, these terms are large because they permit full expression of the large spin-orbit coupling available on the heavy metal center.

The model is readily extended to other systems, and it appears to have considerable validity for the general run of salts of the post-transition metals.¹³ Thus, we believe that the color properties of the post-transition metal salts are obtained by spin-orbit mixing with, and intensity stealing from, charge transfer transitions of anion \rightarrow metal or, less probably, anion \leftarrow metal types.

Acknowledgment. This work was supported by contract between the Department of Energy and the Louisiana State University.

References and Notes

- (1) S. P. McGlynn, T. Azumi, and M. Kinoshita, "Molecular Spectroscopy of Triplet State", Prentice-Hall, Englewood Cliffs, N.J., 1969.
- (2) S. P. McGlynn, *Izv. Akad. Nauk SSSR, Ser. Fiz.*, **37**, 546 (1973); *Bull. Acad. Sci. USSR, Phys. Ser. (Engl. Transl.)*, **79** (1973).
- (3) L. E. Reznik and P. R. Garber, *Opt. Spectrosc.*, **34**, 237 (1973).
- (4) L. E. Reznik, P. R. Garber, and A. V. Fesun, *Sov. Phys. Solid State*, **15**, 2185 (1974).
- (5) L. E. Reznik and L. M. Romyantseva, *Opt. Spectrosc.*, **39**, 509 (1975).
- (6) L. E. Harris, H. J. Maria, and S. P. McGlynn, *Czech. J. Phys. (Engl. Transl.)* **B20**, 1007 (1970).
- (7) A. K. Chandra, N. J. Turro, and A. L. Lyons, *J. Am. Chem. Soc.*, in press.
- (8) N. D. Epitidis, *Angew. Chem., Int. Ed. Engl.*, **13**, 751 (1974).
- (9) T. M. Dunn, *Trans. Faraday Soc.*, **57**, 1441 (1961); B. W. N. Lo, K. M. S. Saxena, and S. Fraga, *Theor. Chim. Acta*, **25**, 97 (1972).
- (10) S. P. McGlynn, L. Vanquickenborne, D. G. Carrol, and M. Kinoshita, "An Introduction to Applied Quantum Chemistry", Holt, Rinehart and Winston, New York, 1972.
- (11) P. Löwdin, *Phys. Rev.*, **97**, 1474 (1955).
- (12) T. F. H. Walker and W. G. Richards, *J. Chem. Phys.*, **52**, 1311 (1970).
- (13) H. Ito and Y. J. I'Haya, *Mol. Phys.*, **24**, 1103 (1972).
- (14) Such situations did not occur in any of the calculations on nitrite salts, but were observed in the case of chlorite salts. Hence, some care must be exercised concerning this point.
- (15) H. Hamaka and L. Goodman, *J. Chem. Phys.*, **42**, 2305 (1965); L. L. Lohr, *ibid.*, **45**, 1362 (1966).
- (16) T. P. Carsey and S. P. McGlynn, to be prepared for publication.
- (17) H. J. Maria, A. Wahborg, and S. P. McGlynn, *J. Chem. Phys.*, **49**, 4925 (1968).
- (18) W. C. Allen and R. N. Dixon, *Trans. Faraday Soc.*, **65**, 1168 (1969).
- (19) R. M. Hochstrasser and A. P. Marchetti, *J. Chem. Phys.*, **50**, 1727 (1969).
- (20) T. P. Myasnikov, L. M. Rabkin, and S. V. Marisova, *Sov. Phys. Solid State*, **5**, 1493 (1974).

- (21) S. J. Strickler and M. Kasha, *J. Am. Chem. Soc.*, **85**, 2899 (1963).
 (22) H. J. Maria, A. T. Armstrong, and S. P. McGlynn, *J. Chem. Phys.*, **50**, 2777 (1969).
 (23) G. B. Carpenter, *Acta Crystallogr.*, **52**, 132 (1952).
 (24) R. E. Long and R. E. Marsh, *Acta Crystallogr.*, **15**, 448 (1962).
 (25) These calculations were similar to those described by Harris et al.⁸ The AO basis was an overlap matched set [L. C. Cusachs, B. I. Trus, D. G. Carroll, and S. P. McGlynn, *J. Chem. Phys.*, **46**, 1532 (1967)]. Spin-orbit coupling constants were taken from Lo et al.⁹ The resulting MOs were finally transformed to a Lowdin-orthogonalized set.
 (26) In this connection, it is notable that a model in which the Ag⁺ ion is situated above the plane of the NO₂⁻ ion induces an x intensity $f_x = 1.61 \times 10^{-4}$.
 (27) J. F. Wyatt, I. H. Hillier, V. R. Saunders, and J. A. Conner, *J. Chem. Phys.*, **54**, 5311 (1971).
 (28) M. Barber, J. A. Conner, I. H. Hillier, and V. R. Saunders, "Electron Spectroscopy", D. A. Shirley, Ed., American Elsevier, New York, 1972, p 379.
 (29) R. Hoffmann, *J. Chem. Phys.*, **39**, 1397 (1963).
 (30) E. Clementi, *J. Chem. Phys.*, **40**, 1944 (1964).
 (31) A. C. Wahl, W. B. England, B. J. Rosenberg, D. G. Hopper, and P. J. Fortune, Argonne National Laboratory Report No. ANL-77-3.

Cooperative Binding of Amine Substrate Molecules by Chiral Europium(III) Shift Reagents

Harry G. Brittain

Contribution from the Department of Chemistry, Ferrum College, Ferrum, Virginia 24088. Received August 13, 1978

Abstract: Various techniques of emission spectroscopy have been used to study the adduct formation of two chiral europium(III) β -diketonate complexes with *n*-propylamine, isopropylamine, *n*-butylamine, *sec*-butylamine, and *tert*-butylamine. The emission intensity of the $^5D_0 \rightarrow ^7F_2$ Eu³⁺ transition was found to be sensitive to the binding of substrate molecules by the lanthanide chelates. It was found that both chelates bound two molecules of amine substrate, and did so in a cooperative fashion. Intermolecular energy transfer from corresponding Tb³⁺ chelates to Eu³⁺ chelates was used to demonstrate that the chelates were not associated in CCl₄ solution, so it was concluded that the cooperative binding of substrates reflects a reorganization of the β -diketonate ligands about the lanthanide ion. Formation constants were calculated for all the adducts formed and it was found that steric effects were important in the binding of substrates by the chiral shift reagents.

Introduction

The usefulness of chiral lanthanide(III) β -diketonate complexes as reagents for the NMR determination of enantiomeric purity has been demonstrated.^{1,2} Eu(III) and Pr(III) chelates of β -diketonates prepared from derivatives of *d*-camphor have received the widest application. Little attention has been paid, however, to the stoichiometry and conformation of the chelate-substrate adducts that actually exist in solution. The crystal structure of the dimethylformamide adduct of Eu(facam)₃ (facam = 3-trifluoroacetyl-*d*-camphorato ion) has been reported,³ but it is not presently clear what relation this crystal structure bears to the actual solution conformation that is of interest to NMR spectroscopists. Until detailed bonding and steric requirements of these chiral lanthanide chelates are better understood, the use of chiral chelates as probes of enantiomeric purity will not be fully understood and the application of theoretical calculations will be severely impeded.

It is well-known that Eu³⁺ complexes of β -diketonates can be highly luminescent, and that this emission is strongly dependent on the geometry of the chelate and on the possible presence of adducts.⁴ Adducts of Eu(dpm)₃ (dpm = 2,2,6,6-tetramethylheptane-3,5-dionato ion) have been studied, and information regarding the association of this achiral shift reagent with some phosphines has been obtained.⁵ Circular polarization of emission (CPE) has been used to study the adduct formation between simple substrates and Eu(facam)₃.⁶ In addition, CPE spectroscopy has been used to examine the adducts formed between achiral Eu³⁺ β -diketonates and chiral substrates.⁷ These studies have shown that emission spectroscopy can be an effective probe of the chelate-substrate complex, and that, under certain conditions, examination of the splittings observed in the sharp lanthanide emission lines

can reveal information regarding the geometry and conformation of the complexes.

In general, emission from a Eu³⁺ β -diketonate chelate is weak if the chelate is dissolved in a noncoordinating solvent and intense if a strongly binding substrate is added to the solution. This observation has made it possible to carry out emission titrations on the achiral Eu³⁺ chelate of 6,6,7,7,8,8,8-heptafluoro-2,2-dimethyloctane-3,5-dione with a variety of substrates.⁸ This study was extended in a subsequent work⁹ in which five achiral chelates were titrated with a variety of simple amine and alcohol substrates. Stoichiometries and formation constants were determined for all adducts in solution, and it was demonstrated that the formation of 1:2 chelate-substrate adducts is fairly widespread within the range of substrates examined.

In the present work, emission titrations have been carried out for Eu(facam)₃ and its more substituted derivative, Eu(hfpc)₃ (hfpc = 3-heptafluoropropylhydroxymethylene-*d*-camphorato ion). The structures of these compounds are shown in Figure 1. In addition, Job's method of continuous variations was used to identify the stoichiometry of the adducts formed in the titrations.

Experimental Section

Eu(facam)₃ and Eu(hfpc)₃ were both purchased from Aldrich. Each complex was sublimed before use, and then dried over P₄O₁₀ in a vacuum desiccator. Spectroquality CCl₄ was used as the solvent in titrations and was dried over molecular sieves before use. Spectrograde *n*-propylamine, isopropylamine, *n*-butylamine, *sec*-butylamine, and *tert*-butylamine were also dried over molecular sieves to ensure that no water was present in any of the samples. All manipulations were carried out in a glovebag under a dry nitrogen atmosphere to prevent possible water contamination. Failure to maintain the rigorous exclusion of water from all solutions resulted in somewhat irreproducible data. Lanthanide chelate concentrations were all kept at 2×10^{-3} M. The titrations were carried out by adding microliter quantities of

* Department of Chemistry, Seton Hall University, South Orange, N.J. 07079.